Potential role of cellular miRNAs in coronavirus-host interplay

Stepan Nersisyan[1], **Narek Engibaryan**[1], **Aleksandra Gorbonos**[1], **Ksenia Kirdey**[1], **Alexey Makhonin**[1], **and Alexander Tonevitsky**[1]

[1]**Faculty of Biology and Biotechnology, Higher School of Economics, Moscow, Russia**

Corresponding author:
Stepan Nersisyan[1]

Email address: snersisyan@hse.ru

ABSTRACT

Host miRNAs are known as important regulators of virus replication and pathogenesis. They can interact with various viruses through several possible mechanisms including direct binding of viral RNA. Identification of human miRNAs involved in coronavirus-host interplay becomes important due to the ongoing COVID-19 pandemic. In this paper we performed computational prediction of high-confidence direct interactions between miRNAs and seven human coronavirus RNAs. As a result, we identified six miRNAs (miR-21-3p, miR-195-5p, miR-16-5p, miR-3065-5p, miR-424-5p and miR-421) with high binding probability across all analyzed viruses. Further bioinformatic analysis of binding sites revealed high conservativity of miRNA binding regions within RNAs of human coronaviruses and their strains. In order to discover the entire miRNA-virus interplay we further analyzed lungs miRNome of SARS-CoV infected mice using publicly available miRNA sequencing data. We found that miRNA miR-21-3p has the largest probability of binding the human coronavirus RNAs and being dramatically up-regulated in mouse lungs during infection induced by SARS-CoV.

INTRODUCTION

Coronavirus disease 2019 (COVID-19) caused by severe acute respiratory syndrome coronavirus 2 (SARS-CoV-2) acquired pandemic status on March 11, 2020 making a dramatic impact on the health of millions of people (Zhou et al., 2020a; Remuzzi and Remuzzi, 2020). Lung failure induced by the acute respiratory distress syndrome (ARDS) is the most common cause of death during viral infection (Xu et al., 2020).

MicroRNAs (miRNAs) are short (22 nucleotides in average) non-coding RNAs which appear to regulate at least one-third of all human protein-coding genes (Nilsen, 2007). Namely, in association with a set of proteins miRNA forms an RNA-induced silencing complex (RISC) and binds 3'-UTR of a target mRNA. The latter promotes translation repression or even mRNA degradation (Carthew and Sontheimer, 2009). Multiple works suggest the critical function of miRNAs in the pathogenesis of various human diseases. Thus, alteration of miRNAs expression is observed during different types of cancer (Di Leva et al., 2014; Shkurnikov et al., 2019), cardiovascular (Schulte et al., 2015; Nouraee and Mowla, 2015) and neurological diseases (Leidinger et al., 2013; Christensen and Schratt, 2009). Other studies have suggested that miRNAs can also participate in intercellular communication (Turchinovich et al., 2019; Baranova et al., 2019).

There are numerous reports consistently demonstrating the role of miRNAs in viral infections. One of the research directions deals with miRNAs which can target viral RNAs. Since RNA of a single-stranded RNA virus (ssRNA virus) is not structurally distinguishable from host mRNA, there are no barriers for miRNA to bind it. In contrast to conventional binding to 3'-UTR of target mRNA, host miRNAs often bind to the coding region or 5'-UTR of viral RNA (Bruscella et al., 2017). Besides translational repression, such interactions can also enhance viral replication or purposefully alter the amount of free miRNAs in a cell (Trobaugh and Klimstra, 2017). For example, miR-122 can bind to 5'-UTR of the hepatitis C virus (HCV) RNA which increases RNA stability and viral replication since it becomes protected from a host exonuclease activity (Shimakami et al., 2012). Another report contains evidence that miR-17 binding

47 sites on RNA of bovine viral diarrhea virus (BVDV) seek to decrease level of free miR-17 in the cell,
48 therefore mediating expression of miRNA targets (Scheel et al., 2016).
49   Other research groups focused on miRNAs altering their expression in response to the viral infection.
50 Specifically, Liu et al. showed that proteins of avian influenza virus H5N1 cause upregulation of miR-
51 200c-3p in the lungs (Liu et al., 2017). This miRNA targets 3'-UTR of *ACE2* mRNA, therefore decreasing
52 its expression. On the other hand, it was shown that decrease in *ACE2* expression is critical in ARDS
53 pathogenesis (Imai et al., 2005). Therefore, H5N1 virus promotes miRNA-mediated *ACE2* silencing to
54 induce ARDS. Recent reports suggest several other host miRNAs which can potentially regulate *ACE2*
55 and *TMPRSS2* expression which can be also important during SARS-CoV-2 infection due to crucial role
56 of these enzymes for virus cell entry (Nersisyan et al., 2020). Another example was given by Choi et al.
57 who studied miRNAs altering their expression during influenza A virus infection (Choi et al., 2014). It
58 was proved that several miRNAs which play an important role in cellular processes, including immune
59 response and cell death, exhibited significant expression differences in infected mice. In the same paper
60 authors show that treatment with the respective anti-miRNAs demonstrates an effective therapeutic action.
61   In recent paper, Fulzele with co-authors found hundreds of miRNAs which can potentially bind to
62 SARS-CoV-2 RNA as well as the RNA of the highly similar SARS-CoV coronavirus (Fulzele et al., 2020).
63 However, this large miRNA list should be narrowed to find high-confidence interactions which should
64 be further experimentally validated. In this work we hypothesized that there can be miRNA-mediated
65 virus-host interplay mechanisms common for several human coronaviruses. For that purpose, we used
66 bioinformatic tools to predict miRNA binding sites within human coronavirus RNAs including ones
67 inducing severe acute respiratory syndrome (SARS-CoV-2, SARS-CoV and MERS-CoV) as well as
68 other human coronaviruses causing common cold, namely, HCoV-OC43, HCoV-NL63, HCoV-HKU1 and
69 HCoV-229E. To find and explore more complex regulatory mechanisms, we also analyzed miRNome of
70 mouse lungs during SARS-CoV infection to find miRNAs whose expression was significantly altered
71 upon viral infection.

MATERIALS AND METHODS

Prediction of miRNA binding sites

74 To find miRNAs which can bind to viral RNAs we used miRDB v6.0 (Chen and Wang, 2020) and
75 TargetScan v7.2 (Agarwal et al., 2015). Target predictions were filtered according to their miRDB target
76 scores, threshold value was set to 75 as in e.g. (Nakano et al., 2019; Zhuang et al., 2019). Viral genomes
77 and their annotations were downloaded from the NCBI Virus (Hatcher et al., 2017) under the following
78 accession numbers:

79   • NC_045512.2 (SARS-CoV-2);
80   • NC_004718.3 (SARS-CoV);
81   • NC_019843.3 (MERS-CoV);
82   • NC_006213.1 (HCoV-OC43);
83   • NC_005831.2 (HCoV-NL63);
84   • NC_006577.2 (HCoV-HKU1);
85   • NC_002645.1 (HCoV-229E).

86   To analyze miRNA-mRNA interactions, we also used miRTarBase v8 (Huang et al., 2020). DIANA-
87 miRPath v3.0 was employed for KEGG pathway analysis (Vlachos et al., 2015).

RNA sequencing data and differential expression analysis

89 MiRNA sequencing (miRNA-seq) data from The Cancer Genome Atlas Lung Adenocarcinoma (TCGA-
90 LUAD) project (Collisson et al., 2014) was used to quantify miRNA expression in the human lungs.
91 Specifically, the said data was downloaded from GDC Data Portal (https://portal.gdc.cancer.gov/) and
92 included miRNA expression table with its columns correspond to 46 normal lung tissues and rows
93 associated with miRNAs (note that only small fraction of TCGA-LUAD cancer samples had analyzed
94 matched normal tissues). We used $\log_2$-transformed Reads Per Million mapped reads (RPM) as a miRNA
95 expression unit.
96   Two miRNA-seq datasets, GSE36971 (Peng et al., 2011) and GSE90624 (Morales et al., 2017), were
97 used to analyze miRNome of SARS-CoV infected mouse lungs (RNA was extracted from homogenized

98 whole lung lobes). Raw FASTQ files were downloaded from the Sequence Read Archive (Leinonen et al.,
99 2011). Adapters were trimmed via Cutadapt 2.10 (Martin, 2011), miRNA expression was quantified by
100 miRDeep2 (Friedländer et al., 2012) using GRCm38.p6 mouse genome (release M25) from GENCODE
101 (Frankish et al., 2019) and miRBase 22.1 (Kozomara et al., 2019). Gene expression profile of SARS-CoV
102 infected mouse lungs was downloaded in form of count matrix from the Gene Expression Omnibus (GEO)
103 (Barrett et al., 2013) under GSE52405 accession number (Josset et al., 2014). Differential expression
104 analysis was performed with DESeq2 (Love et al., 2014). The results were filtered using 0.05 threshold
105 on adjusted p-value and 1.5 on fold change (linear scale).

Sequence alignment

107 Multiple Sequence Alignment (MSA) of viral genomic sequences was done using Kalign 2.04 (Lassmann
108 et al., 2009). Two MSA series were performed. In the first one we aligned seven human coronavirus
109 genomes. In the second one different coronavirus strains were aligned for each of analyzed viruses. All
110 genomes available on the NCBI Virus were used for SARS-CoV, MERS-CoV, HCoV-OC43, HCoV-NL63,
111 HCoV-HKU1 and HCoV-229E (263, 253, 139, 58, 39 and 28 genomes, respectively). For SARS-CoV-2
112 thousand genomes were randomly selected to preserve the percentage of samples from each country.
113 GISAID clade annotation (Elbe and Buckland-Merrett, 2017) was obtained for 956 SARS-CoV-2 genomes
114 (annotation was missing for other genomes). For each virus we established the mapping between alignment
115 and genomic coordinates. With the use of this mapping, miRNA seed region binding positions within
116 viral RNAs were placed on the alignment.

Data and code availability

118 All code was written in Python 3 programming language with extensive use of NumPy (Van Der Walt
119 et al., 2011) and Pandas (McKinney, 2010) modules. Statistical analysis was performed using the SciPy
120 stats (Virtanen et al., 2020), plots were constructed using the Seaborn and Matplotlib (Hunter, 2007).
121 MSA was visualized using Unipro UGENE (Okonechnikov et al., 2012). All used data and source codes
122 are available on GitHub (https://github.com/s-a-nersisyan/host-miRNAs-vs-coronaviruses).

RESULTS

Human coronavirus RNAs have numerous common host miRNA binding sites

125 To identify human miRNAs that may bind to RNAs of human coronaviruses we used two classical
126 miRNA target prediction tools: miRDB and TargetScan. TargetScan results can be ranked with different
127 seed-region binding types while miRDB results can be ranked with so-called "target score" associated
128 with the probability of successful binding. Interestingly, for each of viruses TargetScan predicted 2-3 times
129 higher number of miRNAs, while 80-85% miRNAs predicted by miRDB were predicted by TargetScan
130 too (for the summary on the number of miRNAs predicted for each of viral genomes see Table S1).
131   We made a list of 19 miRNAs potentially targeting multiple viral RNAs by selecting miRNAs with
132 miRDB target scores greater than 75 in all analyzed viruses (Table S2). For further analysis, we selected
133 only high confidence miRNAs according to miRBase, namely, hsa-miR-21-3p, hsa-miR-195-5p, hsa-miR-
134 16-5p, hsa-miR-3065-5p, hsa-miR-424-5p and hsa-miR-421. According to TargetScan, all "guide" strand
135 miRNAs except hsa-miR-3065-5p were conserved among species including miR-16-5p/195-5p/424-5p
136 family with the shared seed sequence. Despite being a "passenger" strand, hsa-miR-21-3p was shown to
137 be functionally active and conserved over the mammalian evolution (Báez-Vega et al., 2016; Lo et al.,
138 2013). For target scores of selected miRNAs as well as corresponding hierarchical clustering of viruses
139 see Figure 1A. As it can be seen, such clustering grouped together SARS-CoV and SARS-CoV-2 as well
140 as HCoV-229E and HCoV-NL63 which can be also observed when clustering is performed based on viral
141 genomic sequences similarity (Zhou et al., 2020b).
142   Six identified miRNAs showed similar functional patterns. Namely, KEGG pathway analysis of exper-
143 imentally validated target genes revealed 54 enriched terms including pathways involved in pathogenesis
144 of lung and several other cancers, viral infections as well as signaling pathways such as p53, TGF-β and
145 FoxO (see Table S3). In order to assess which of these miRNAs could demonstrate activity in human
146 lungs, we analyzed miRNA-seq data from TCGA-LUAD project. Two of the said miRNAs demonstrated
147 relatively high expression (see Figure 1B). Specifically, hsa-miR-21-3p and hsa-miR-16-5p corresponded
148 to top-5% of highly expressed miRNAs according to their mean expression level taken across all samples.
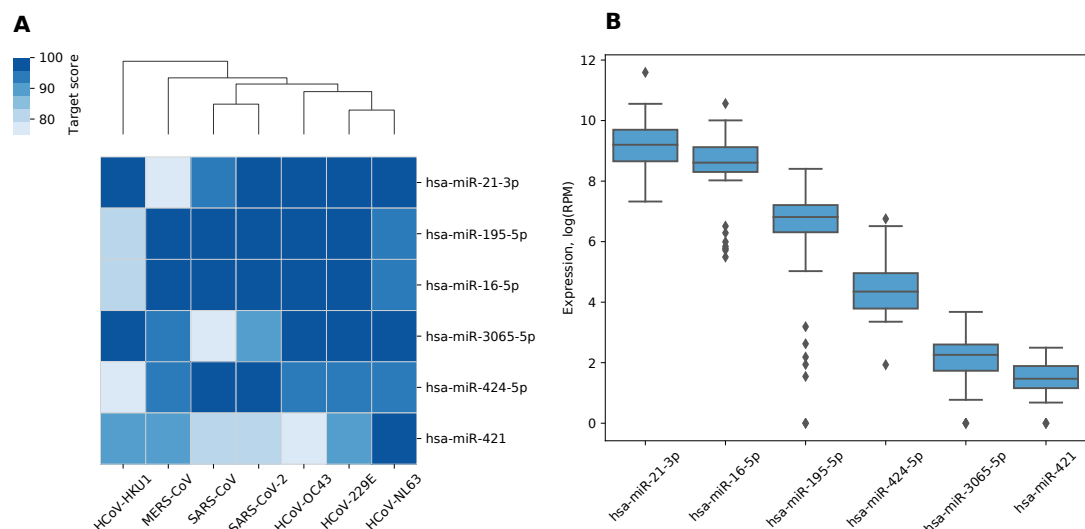
Figure 1. miRNAs with the highest target scores. (A) Hierarchical clustering of coronaviruses based on miRDB target scores. Rows are sorted according to the mean target score. (B) Expression distribution of miRNAs in human lungs.

Viral binding sites of miRNAs are conserved across different coronaviruses and their strains

Each of identified miRNAs had dozens of binding regions within analyzed viral RNAs (see Table S4). Interestingly, the peak number of hsa-miR-16-5p/195-5p/424-5p binding positions fell on SARS-CoV and SARS-CoV-2, while for other miRNAs the most enriched virus was HCoV-NL63. To go deeper and analyze mutual arrangement of these sites we performed multiple sequence alignment on seven analyzed genomes and mapped the predicted miRNA binding positions from individual genomes to the obtained alignment. Further, for each binding site mapped to the alignment we calculated a number of viruses sharing that particular miRNA binding site. Positions common for two or more viruses were utilized in the downstream analysis.

In general, different miRNAs demonstrated dissimilar patterns of viral binding regions (for summary information see Table 1). In particular, hsa-miR-21-3p and hsa-miR-421 had positions on the alignment specific to six out of seven considered coronaviruses (see Figure 2). Two most enriched binding positions of hsa-miR-16-5p/195-5p/424-5p family were common for five viruses, while maximum number of viruses sharing binding regions of hsa-miR-3065-5p was equal to three. Interestingly, most binding sites obtained for all considered miRNAs were found within nonstructural proteins located in polyprotein 1ab coding region (89%), about 8% of positions were located within spike protein while the rest was spread over N and M proteins. Detailed information is given in Table S5.

	2	3	4	5	6	Total
hsa-miR-21-3p	24	6	2	1	1	34
hsa-miR-16-5p/195-5p/424-5p	16	5	0	2	0	23
hsa-miR-3065-5p	41	11	0	0	0	52
hsa-miR-421	34	3	2	2	1	42

Table 1. Number of common miRNA binding sites on coronavirus RNAs. Column names refer to the number of viruses sharing a miRNA binding region.

To group coronaviruses based on the probability of sharing common miRNA binding positions, we calculated the number of matching positions in the alignment for each miRNA and pair of viruses (see Figure S1). Then, per each miRNA this data was normalized by the overall number of binding positions shared by two or more viruses, and used as a distance matrix for hierarchical clustering (see Figure 3). Interestingly, for majority of miRNAs such clustering was completely similar to that of viruses based on

A
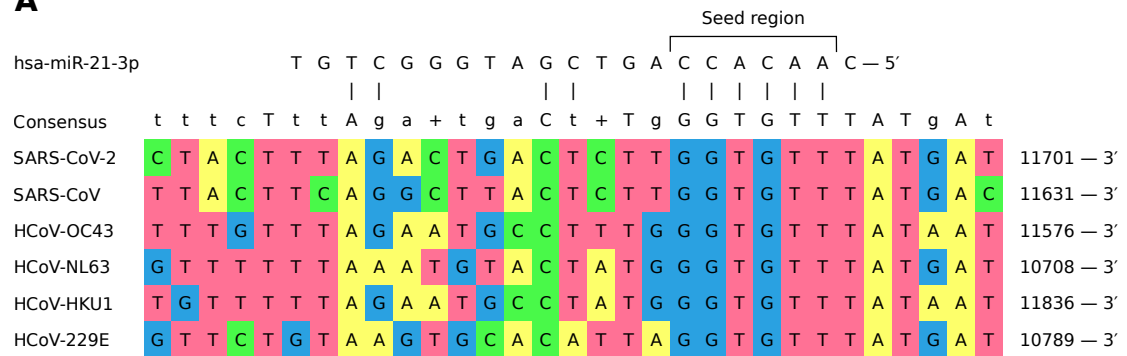
B
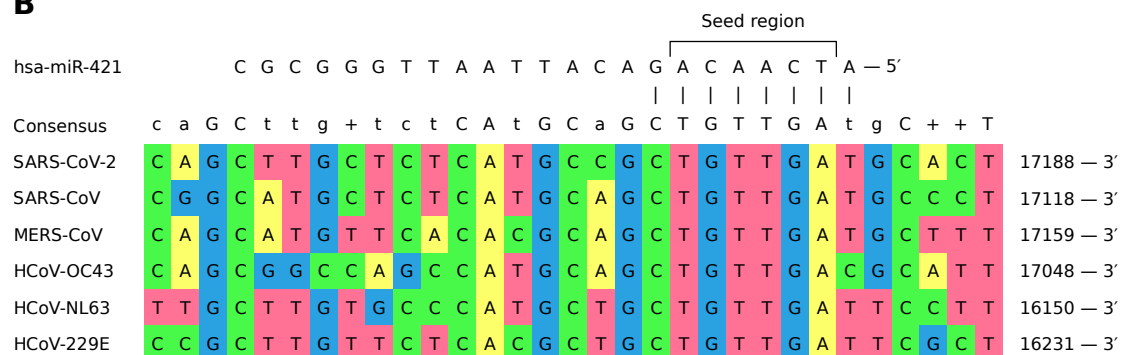
Figure 2. **Shared binding sites of hsa-miR-21-3p and hsa-miR-421 on human coronavirus RNAs.** (A) hsa-miR-21-3p. (B) hsa-miR-421.

their genomic sequence similarity (Zhou et al., 2020b).

In order to assess conservativity of miRNA binding regions across viral strains, we performed multiple sequence alignment of available viral genomes per each human coronavirus independently. The results revealed high conservativity of these regions: 59% to 98% of binding sites within coronavirus RNAs had no mutation, while mean of average mutation rates (i.e. number of mutations normalized by region length and number of strains) across all viruses varied from 0.3% to 0.7% (see Table S4). Interestingly, there were no mutations for each of viruses in aforementioned hsa-miR-21-3p binding site shared by six coronaviruses, while HCoV-OC43 mutation rate was equal to 1% in the similar hsa-miR-421 site. Exact values of average mutation rates are given in Table S6. Finally, we assessed mutation rates within seven SARS-CoV-2 clades introduced by GISAID. Binding sites of hsa-miR-21-3p and hsa-miR-421 had mismatches only within GH and S clades, sites of hsa-miR-3065-5p were mutated in GH and GR clades, while binding regions of hsa-miR-16-5p/195-5p/424-5p family showed mutations in all clades except O (see Table 2).

	G	GH	GR	L	O	S	V
hsa-miR-21-3p	0	0.007%	0	0	0	0.03%	0
hsa-miR-16-5p/195-5p/424-5p	0.01%	0.03%	0.01%	0.02%	0	0.05%	0.08%
hsa-miR-3065-5p	0	0.02%	0.01%	0	0	0	0
hsa-miR-421	0	0.003%	0	0	0	0.01%	0

Table 2. Mean of average mutation rates in miRNA binding sites across SARS-CoV-2 clades.
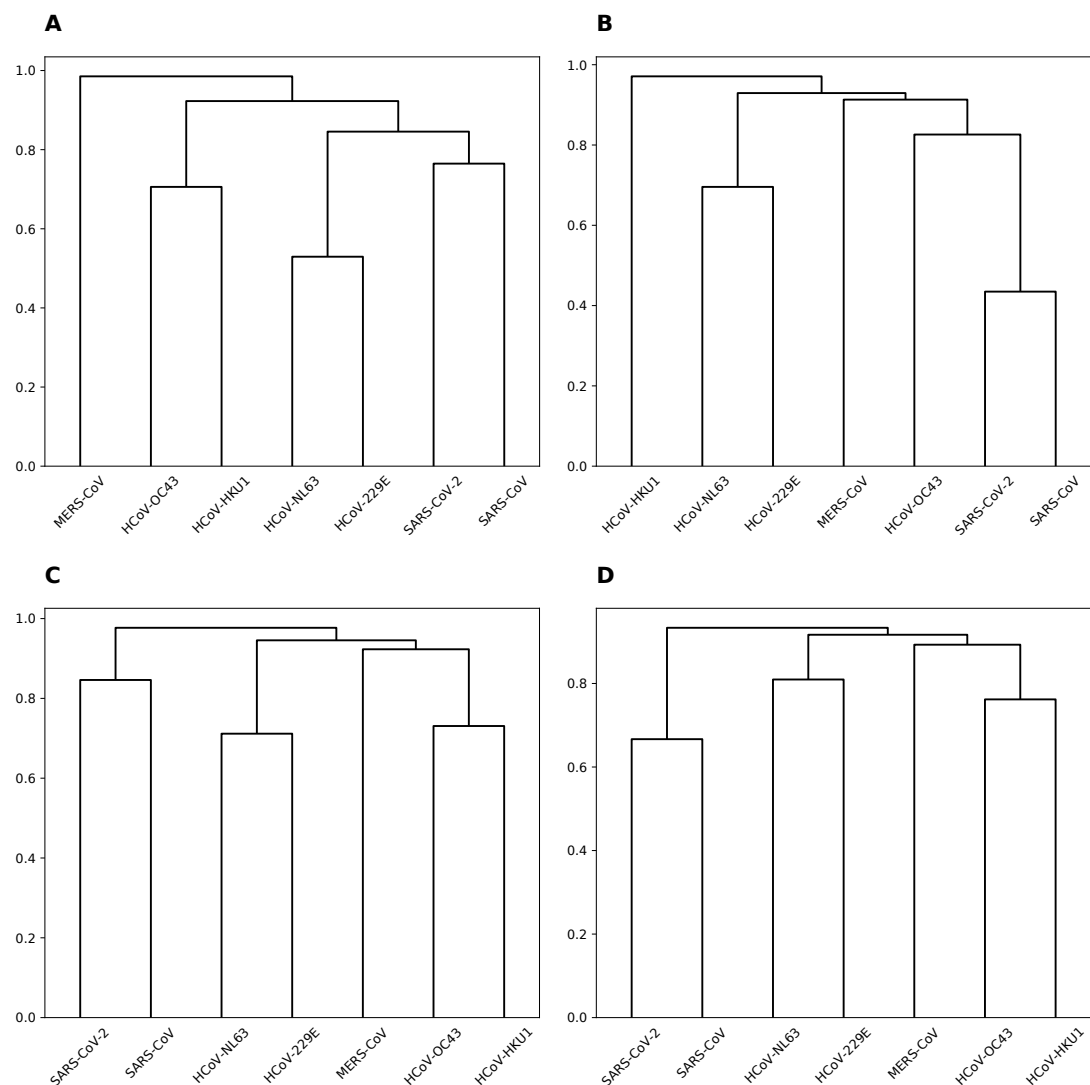
Figure 3. Hierarchical clustering of human coronaviruses based on the number of shared binding sites. (A) hsa-miR-21-3p. (B) hsa-miR-16-5p/195-5p/424-5p. (C) hsa-miR-3065-5p. (D) hsa-miR-421.

MiR-21 and its target genes exhibit significant expression alteration in mouse lungs during SARS-CoV infection

To further explore a potential interplay between host miRNAs and coronaviruses, we hypothesized that some of miRNAs predicted to bind viral RNAs can have altered expression during the infection. In order to verify this hypothesis, we analyzed two publicly available miRNA-seq datasets of mouse lungs during SARS-CoV infection. The first dataset (GSE36971) included data derived from four mouse strains infected by SARS-CoV and four corresponding control mice. The second dataset (GSE90624) comprised three infected and four control mice.

Differential expression analysis revealed 19 miRNAs in the first dataset and 21 in the second dataset where expression change during infection was statistically significant (see Table S7). Six miRNAs were differentially expressed in both datasets, five of them had matched fold change signs, namely, were overexpressed in infected mice (see Figure 4). This was a statistically significant overlap since an estimate of the probability for 19- and 21-element random miRNA sets having five or more common elements was equal to 4.07×10^{-7} (hypergeometric test). Surprisingly, miR-21a-3p which we previously identified as a potential regulator of all analyzed coronavirus genomes with one of the highest scores exhibited

8.3-fold increase (adjusted $p = 5.72 \times 10^{-35}$) and 11-fold increase (adjusted $p = 5.77 \times 10^{-11}$) during SARS-CoV infection in the first and the second datasets, respectively.
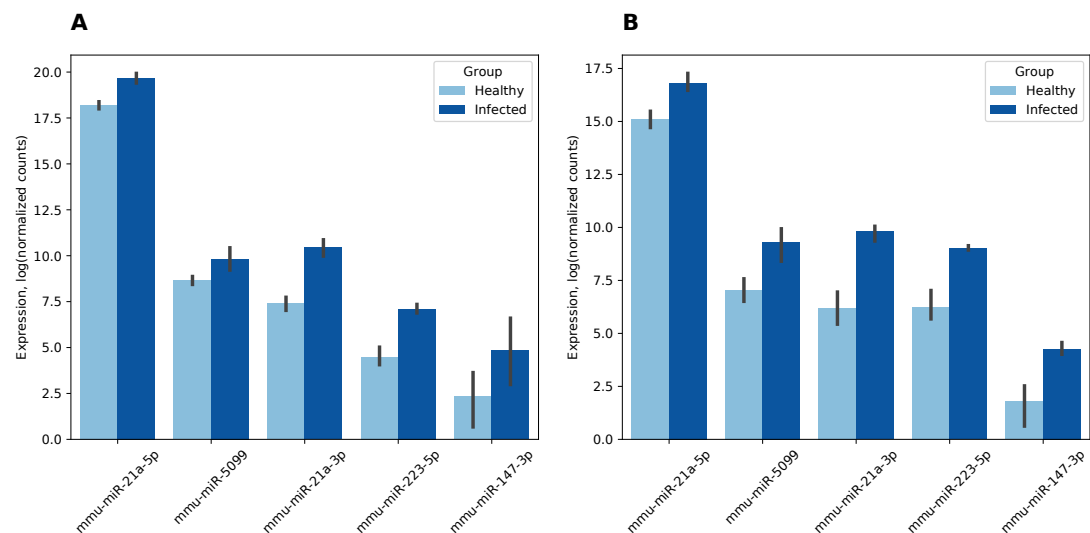
Figure 4. Differentially expressed mouse lung miRNAs. (A) GSE36971. (B) GSE90624. Differential expression analysis was performed using DESeq2. Note that counts were normalized independently per each dataset. Thus, presented values should not be directly compared across (A) and (B). Vertical lines on the bar top indicate 95% confidence intervals.

Expression of mmu-miR-21a-5p (the opposite "guide" strand of the same hairpin) was also increased in the infected group (2.8- and 3.2-folds, respectively). The latter had a particular importance since mmu-miR-21a-5p was highly expressed in mice during both experiments. Namely, according to its mean expression across all samples it was 4th and 38th out of 2302 in the first and the second datasets, respectively. Thus, significant expression change of this miRNA can dramatically affect expression of its target genes.

In order to capture aberrant expression of miRNA target genes during infection, we analyzed RNA sequencing (RNA-seq) data of eight SARS-CoV infected mice strains published by the same group of authors as in the first miRNA-seq dataset (GSE52405). Two strategies were pursued to generate a list of miRNA targets. Namely, we used target prediction tools described in the previous section as well as literature-curated miRTarBase database.

First, we took genes predicted both by miRDB and TargetScan with miRDB target score greater than 75. Additionally, we thresholded this list using top-10% predictions based on TargetScan's cumulative weighted context++ score. A significant fraction of mmu-miR-21a-5p target genes were down-regulated during the infection. Namely, 6 out of 24 considered genes demonstrated significant decrease in expression (hypergeometric test $p = 7.6 \times 10^{-3}$). For four other miRNAs, there was no statistical significance on the number of down-regulated target genes. The situation was quite different for interactions enlisted in miRTarBase. Thus, 2 out of 2 mmu-miR-21a-3p target genes (*Snca* and *Reck*) were down-regulated (hypergeometric test $p = 5.7 \times 10^{-3}$), while only 6 out of 37 mmu-miR-21a-5p target genes exhibited expression decrease (hypergeometric test $p = 0.057$). As in the previous case, no significant number of down-regulated target genes was observed for other miRNAs.

DISCUSSION

In this paper we identified several cellular miRNAs (miR-21-3p, miR-16-5p/195-5p/424-5p, miR-3065-5p and miR-421) potentially regulating all human coronaviruses via direct binding to viral RNAs. Moreover, aside from virus specific binding sites we identified genomic positions which can serve as conserved targets for putative miRNAs. As one can expect, viruses with high genomic similarity such as SARS-CoV-2 / SARS-CoV or HCoV-229E / HCoV-NL63 had higher number of shared binding sites. Similar computational approach to discover direct miRNA-virus interactions was already employed by Fulzele

et al (Fulzele et al., 2020). Namely, using miRDB researchers predicted miRNAs targeting RNAs of SARS-CoV-2 and SARS-CoV. Despite large intersection of predicted miRNA sets, in the present paper we focused on miRNAs targeting as much human coronavirus RNAs as possible, which resulted in different lists of "top" miRNAs.

Several hypotheses can be put forward to explain biological motivation of direct host miRNA-virus interactions. At first sight, one can think about host miRNA-mediated immune response to the viral infection. For example, translation of human T cell leukemia virus type I (HTLV-1) is inhibited by miR-28-3p activity (Bai and Nicot, 2015). However, our results suggest that binding sites of identified miRNAs are actually conserved across human coronaviruses. Thus, viruses can purposefully accumulate host miRNA binding sites to slow down their own replication rate in order to evade fast detection and elimination by the immune system. Such behaviour was reported e.g. in the case of eastern equine encephalitis virus (EEEV) (Trobaugh et al., 2014). Authors reported that haematopoietic-cell-specific miRNA miR-142-3p directly binds viral RNA which limits the replication of virus thereby suppressing innate immunity. The latter was shown to be crucial in the virus infection pathogenesis.

Functional activity of identified miRNAs was already referred to in the context of viral infections. Thus, it was proved that miR-21-3p regulates the replication of influenza A virus (IAV) (Xia et al., 2018). Namely, hsa-miR-21-3p targeting 3'-UTR of *HDAC8* gene was shown to be down-regulated during IAV infection of human alveolar epithelial cell line A549 using both miRNA microarray and quantitative PCR analysis. Consecutive increase in the *HDAC8* expression was shown to promote viral replication. Another report highlights the role of miR-16-5p in pathogenesis of Enterovirus 71 (EV71) infection (Zheng et al., 2017). In particular, authors validated EV71-induced expression of miR-16-5p and found that this miRNA can inhibit EV71 replication *in vitro* and *in vivo* by targeting *CCNE1* and *CCND1* genes.

Remarkably, we found that expression of miR-21-3p in mice lungs exhibits a 8-fold increase upon SARS-CoV infection. Interestingly, miR-21-5p (the "guide" strand of the same pre-miRNA hairpin) demonstrated only a 3-fold increase in expression. To explain this phenomena of non-symmetrical expression increase, we hypothesize that binding to the viral genome saves star miRNA miR-21-3p from degradation after unsuccessful attempt of AGO2 loading. A similar mechanism was already mentioned in several papers. Namely, Janas with co-authors demonstrated that Ago-free miRNAs can escape degradation by forming Ago-free miRNA-mRNA duplex (Janas et al., 2012). Another concept was named as target RNA directed miRNA degradation (TDMD) and consists of the fact that highly complementary target RNA can trigger miRNA degradation by a mechanism involving nucleotide addition and exonucleolytic degradation (la Mata et al., 2015; Zhang et al., 2019). Thus, non-proportional up-regulation of miR-21 arms can be indirect evidence that miR-21-3p directly targets the viral RNA or that the miR-21-5p is being actively degraded during target mRNA binding.

CONCLUSIONS

Several miRNAs having potential of direct interactions with human coronaviruses were discovered in this paper. While a majority of them were virus-specific, some miRNAs were shown to target all analyzed viral RNAs. Exploration of publicly available miRNomic data of SARS-CoV infected mice lungs revealed that one of these miRNAs (miR-21-3p) demonstrated a dramatic expression increase upon infection. Taking into account high structural similarity of SARS-CoV and SARS-CoV-2 including common miR-21-3p binding sites as well as the fact that this miRNA is also expressed in human lungs, the obtained results open new opportunities in understanding COVID-19 pathogenesis and consecutive development of therapeutic approaches.

ACKNOWLEDGMENTS

The authors thank Dr. Maxim Shkurnikov for valuable comments and discussions.

REFERENCES

Agarwal, V., Bell, G. W., Nam, J. W., and Bartel, D. P. (2015). Predicting effective microRNA target sites in mammalian mRNAs. *Elife*, 4.

Báez-Vega, P. M., Vargas, I. M., Valiyeva, F., Rosado, J. E., Roman, A., Flores, J., Marcos-Martínez, M. J., and Vivas-Mejía, P. E. (2016). Targeting miR-21-3p inhibits proliferation and invasion of ovarian cancer cells. *Oncotarget*, 7(24):36321–36337.

281 Bai, X. T. and Nicot, C. (2015). MiR-28-3p is a cellular restriction factor that inhibits human T cell
282   leukemia virus, type 1 (HTLV-1) replication and virus infection. *J. Biol. Chem.*, 290(9):5381–5390.

283 Baranova, A., Maltseva, D., and Tonevitsky, A. (2019). Adipose may actively delay progression of NAFLD
284   by releasing tumor-suppressing, anti-fibrotic miR-122 into circulation. *Obes. Rev.*, 20(1):108–118.

285 Barrett, T., Wilhite, S. E., Ledoux, P., Evangelista, C., Kim, I. F., Tomashevsky, M., Marshall, K. A.,
286   Phillippy, K. H., Sherman, P. M., Holko, M., et al. (2013). NCBI GEO: Archive for functional genomics
287   data sets - Update. *Nucleic Acids Res.*, 41(D1):D991–5.

288 Bruscella, P., Bottini, S., Baudesson, C., Pawlotsky, J. M., Feray, C., and Trabucchi, M. (2017). Viruses
289   and miRNAs: More friends than foes. *Front. Microbiol.*, 8:824.

290 Carthew, R. W. and Sontheimer, E. J. (2009). Origins and Mechanisms of miRNAs and siRNAs. *Cell*,
291   136(4):642–655.

292 Chen, Y. and Wang, X. (2020). MiRDB: An online database for prediction of functional microRNA
293   targets. *Nucleic Acids Res.*, 48(D1):D127–D131.

294 Choi, E. J., Kim, H. B., Baek, Y. H., Kim, E. H., Pascua, P. N. Q., Park, S. J., Kwon, H. I., Lim, G. J.,
295   Kim, S., Kim, Y. I., et al. (2014). Differential microRNA expression following infection with a
296   mouse-adapted, highly virulent avian H5N2 virus. *BMC Microbiol.*, 14(1):252.

297 Christensen, M. and Schratt, G. M. (2009). microRNA involvement in developmental and functional
298   aspects of the nervous system and in neurological diseases. *Neurosci. Lett.*, 466(2):55–62.

299 Collisson, E. A., Campbell, J. D., Brooks, A. N., Berger, A. H., Lee, W., Chmielecki, J., Beer, D. G.,
300   Cope, L., Creighton, C. J., Danilova, L., et al. (2014). Comprehensive molecular profiling of lung
301   adenocarcinoma: The cancer genome atlas research network. *Nature*, 511(7511):543–550.

302 Di Leva, G., Garofalo, M., and Croce, C. M. (2014). MicroRNAs in Cancer. *Annu. Rev. Pathol. Mech.*
303   *Dis.*, 9(1):287–314.

304 Elbe, S. and Buckland-Merrett, G. (2017). Data, disease and diplomacy: GISAID's innovative contribution
305   to global health. *Glob. Challenges*, 1(1):33–46.

306 Frankish, A., Diekhans, M., Ferreira, A. M., Johnson, R., Jungreis, I., Loveland, J., Mudge, J. M., Sisu,
307   C., Wright, J., Armstrong, J., et al. (2019). GENCODE reference annotation for the human and mouse
308   genomes. *Nucleic Acids Res.*, 47(D1):D766–D773.

309 Friedländer, M. R., MacKowiak, S. D., Li, N., Chen, W., and Rajewsky, N. (2012). MiRDeep2 accurately
310   identifies known and hundreds of novel microRNA genes in seven animal clades. *Nucleic Acids Res.*,
311   40(1):37–52.

312 Fulzele, S., Sahay, B., Yusufu, I., Lee, T. J., Sharma, A., Kolhe, R., and Isales, C. M. (2020). COVID-19
313   Virulence in Aged Patients Might Be Impacted by the Host Cellular MicroRNAs Abundance/Profile.
314   *Aging Dis.*, 11(3):509.

315 Hatcher, E. L., Zhdanov, S. A., Bao, Y., Blinkova, O., Nawrocki, E. P., Ostapchuck, Y., Schaffer, A. A.,
316   and Rodney Brister, J. (2017). Virus Variation Resource-improved response to emergent viral outbreaks.
317   *Nucleic Acids Res.*, 45(D1):D482–D490.

318 Huang, H. Y., Lin, Y. C. D., Li, J., Huang, K. Y., Shrestha, S., Hong, H. C., Tang, Y., Chen, Y. G., Jin, C. N.,
319   Yu, Y., et al. (2020). MiRTarBase 2020: Updates to the experimentally validated microRNA-target
320   interaction database. *Nucleic Acids Res.*, 48(D1):D148–D154.

321 Hunter, J. D. (2007). Matplotlib: A 2D graphics environment. *Comput. Sci. Eng.*, 9(3):99–104.

322 Imai, Y., Kuba, K., Rao, S., Huan, Y., Guo, F., Guan, B., Yang, P., Sarao, R., Wada, T., Leong-Poi,
323   H., et al. (2005). Angiotensin-converting enzyme 2 protects from severe acute lung failure. *Nature*,
324   436(7047):112–116.

325 Janas, M. M., Wang, B., Harris, A. S., Aguiar, M., Shaffer, J. M., Subrahmanyam, Y. V., Behlke, M. A.,
326   Wucherpfennig, K. W., Gygi, S. P., Gagnon, E., et al. (2012). Alternative RISC assembly: Binding and
327   repression of microRNA-mRNA duplexes by human Ago proteins. *RNA*, 18(11):2041–2055.

328 Josset, L., Tchitchek, N., Gralinski, L. E., Ferris, M. T., Eisfeld, A. J., Green, R. R., Thomas, M. J.,
329   Tisoncik-Go, J., Schroth, G. P., Kawaoka, Y., et al. (2014). Annotation of long non-coding RNAs
330   expressed in Collaborative Cross founder mice in response to respiratory virus infection reveals a new
331   class of interferon-stimulated transcripts. *RNA Biol.*, 11(7):875–890.

332 Kozomara, A., Birgaoanu, M., and Griffiths-Jones, S. (2019). MiRBase: From microRNA sequences to
333   function. *Nucleic Acids Res.*, 47(D1):D155–D162.

334 la Mata, M., Gaidatzis, D., Vitanescu, M., Stadler, M. B., Wentzel, C., Scheiffele, P., Filipowicz, W., and
335   Großhans, H. (2015). Potent degradation of neuronal miRNA s induced by highly complementary

336   targets . *EMBO Rep.*, 16(4):500–511.

337   Lassmann, T., Frings, O., and Sonnhammer, E. L. (2009). Kalign2: High-performance multiple alignment
338   of protein and nucleotide sequences allowing external features. *Nucleic Acids Res.*, 37(3):858–865.

339   Leidinger, P., Backes, C., Deutscher, S., Schmitt, K., Mueller, S. C., Frese, K., Haas, J., Ruprecht, K.,
340   Paul, F., Stähler, C., et al. (2013). A blood based 12-miRNA signature of Alzheimer disease patients.
341   *Genome Biol.*, 14(7):R78.

342   Leinonen, R., Sugawara, H., and Shumway, M. (2011). The sequence read archive. *Nucleic Acids Res.*,
343   39:D19–21.

344   Liu, Q., Du, J., Yu, X., Xu, J., Huang, F., Li, X., Zhang, C., Li, X., Chang, J., Shang, D., et al. (2017).
345   MiRNA-200c-3p is crucial in acute respiratory distress syndrome. *Cell Discov.*, 3:17021.

346   Lo, T. F., Tsai, W. C., and Chen, S. T. (2013). MicroRNA-21-3p, a Berberine-Induced miRNA, Directly
347   Down-Regulates Human Methionine Adenosyltransferases 2A and 2B and Inhibits Hepatoma Cell
348   Growth. *PLoS One*, 8(9).

349   Love, M. I., Huber, W., and Anders, S. (2014). Moderated estimation of fold change and dispersion for
350   RNA-seq data with DESeq2. *Genome Biol.*, 15(12):550.

351   Martin, M. (2011). Cutadapt removes adapter sequences from high-throughput sequencing reads. *EMB-*
352   *net.journal*, 17(1):10.

353   McKinney, W. (2010). Data structures for statistical computing in Python. *Proceedings of the 9th Python*
354   *in science conference*, pages 56–61.

355   Morales, L., Oliveros, J. C., Fernandez-Delgado, R., TenOever, B. R., Enjuanes, L., and Sola, I. (2017).
356   SARS-CoV-Encoded Small RNAs Contribute to Infection-Associated Lung Pathology. *Cell Host*
357   *Microbe*, 21(3):344–355.

358   Nakano, Y., Yoshimoto, T., Watanabe, R., Murakami, M., Fukuda, T., Saito, K., Fujii, Y., Akashi, T.,
359   Tanaka, T., Yamada, T., et al. (2019). MiRNA299 involvement in CYP11B2 expression in aldosterone-
360   producing adenoma. *Eur. J. Endocrinol.*, 181(1):69–78.

361   Nersisyan, S., Shkurnikov, M., Turchinovich, A., Knyazev, E., and Tonevitsky, A. (2020). Integrative
362   analysis of miRNA and mRNA sequencing data reveals potential regulatory mechanisms of ACE2 and
363   TMPRSS2. *PLoS One*, 15(7):e0235987.

364   Nilsen, T. W. (2007). Mechanisms of microRNA-mediated gene regulation in animal cells. *Trends Genet.*,
365   23(5):243–249.

366   Nouraee, N. and Mowla, S. J. (2015). miRNA therapeutics in cardiovascular diseases: Promises and
367   problems. *Front. Genet.*, 6:232.

368   Okonechnikov, K., Golosova, O., Fursov, M., Varlamov, A., Vaskin, Y., Efremov, I., German Grehov,
369   O. G., Kandrov, D., Rasputin, K., Syabro, M., et al. (2012). Unipro UGENE: A unified bioinformatics
370   toolkit. *Bioinformatics*, 28(8):1166–1167.

371   Peng, X., Gralinski, L., Ferris, M. T., Frieman, M. B., Thomas, M. J., Proll, S., Korth, M. J., Tisoncik, J. R.,
372   Heise, M., Luo, S., et al. (2011). Integrative deep sequencing of the mouse lung transcriptome reveals
373   differential expression of diverse classes of small RNAs in response to respiratory virus infection.
374   *MBio*, 2(6).

375   Remuzzi, A. and Remuzzi, G. (2020). COVID-19 and Italy: what next? *Lancet*, 395(10231):1225–1228.

376   Scheel, T. K., Luna, J. M., Liniger, M., Nishiuchi, E., Rozen-Gagnon, K., Shlomai, A., Auray, G., Gerber,
377   M., Fak, J., Keller, I., et al. (2016). A Broad RNA Virus Survey Reveals Both miRNA Dependence and
378   Functional Sequestration. *Cell Host Microbe*, 19(3):409–423.

379   Schulte, C., Molz, S., Appelbaum, S., Karakas, M., Ojeda, F., Lau, D. M., Hartmann, T., Lackner, K. J.,
380   Westermann, D., Schnabel, R. B., et al. (2015). MiRNA-197 and miRNA-223 predict cardiovascular
381   death in a cohort of patients with symptomatic coronary artery disease. *PLoS One*, 10(12):e0145930.

382   Shimakami, T., Yamane, D., Jangra, R. K., Kempf, B. J., Spaniel, C., Barton, D. J., and Lemon, S. M.
383   (2012). Stabilization of hepatitis C virus RNA by an Ago2-miR-122 complex. *Proc. Natl. Acad. Sci. U.*
384   *S. A.*, 109(3):941–946.

385   Shkurnikov, M., Nikulin, S., Nersisyan, S., Poloznikov, A., Zaidi, S., Baranova, A., Schumacher, U.,
386   Wicklein, D., and Tonevitsky, A. (2019). LAMA4-Regulating miR-4274 and Its Host Gene SORCS2
387   Play a Role in IGFBP6-Dependent Effects on Phenotype of Basal-Like Breast Cancer. *Front. Mol.*
388   *Biosci.*, 6:122.

389   Trobaugh, D. W., Gardner, C. L., Sun, C., Haddow, A. D., Wang, E., Chapnik, E., Mildner, A., Weaver,
390   S. C., Ryman, K. D., and Klimstra, W. B. (2014). RNA viruses can hijack vertebrate microRNAs to

391   suppress innate immunity. *Nature*, 506(7487):245–248.

392 Trobaugh, D. W. and Klimstra, W. B. (2017). MicroRNA Regulation of RNA Virus Replication and
393   Pathogenesis. *Trends Mol. Med.*, 23(1):80–93.

394 Turchinovich, A., Drapkina, O., and Tonevitsky, A. (2019). Transcriptome of extracellular vesicles:
395   State-of-the-art. *Front. Immunol.*, 10.

396 Van Der Walt, S., Colbert, S. C., and Varoquaux, G. (2011). The NumPy array: A structure for efficient
397   numerical computation. *Comput. Sci. Eng.*, 13(2):22–30.

398 Virtanen, P., Gommers, R., Oliphant, T. E., Haberland, M., Reddy, T., Cournapeau, D., Burovski, E.,
399   Peterson, P., Weckesser, W., Bright, J., et al. (2020). SciPy 1.0: fundamental algorithms for scientific
400   computing in Python. *Nat. Methods*, 17(3):261–272.

401 Vlachos, I. S., Zagganas, K., Paraskevopoulou, M. D., Georgakilas, G., Karagkouni, D., Vergoulis, T.,
402   Dalamagas, T., and Hatzigeorgiou, A. G. (2015). DIANA-miRPath v3.0: Deciphering microRNA
403   function with experimental support. *Nucleic Acids Res.*, 43(W1):W460–W466.

404 Xia, B., Lu, J., Wang, R., Yang, Z., Zhou, X., and Huang, P. (2018). miR-21-3p regulates Influenza A
405   virus replication by targeting Histone deacetylase-8. *Front. Cell. Infect. Microbiol.*, 8:175.

406 Xu, Z., Shi, L., Wang, Y., Zhang, J., Huang, L., Zhang, C., Liu, S., Zhao, P., Liu, H., Zhu, L., et al. (2020).
407   Pathological findings of COVID-19 associated with acute respiratory distress syndrome. *Lancet Respir.*
408   *Med.*, 8(4):420–422.

409 Zhang, Z., Pi, J., Zou, D., Wang, X., Xu, J., Yu, S., Zhang, T., Li, F., Zhang, X., Zhao, H., et al. (2019).
410   microRNA arm-imbalance in part from complementary targets mediated decay promotes gastric cancer
411   progression. *Nat. Commun.*, 10(1):4397.

412 Zheng, C., Zheng, Z., Sun, J., Zhang, Y., Wei, C., Ke, X., Liu, Y., Deng, L., and Wang, H. (2017). MiR-
413   16-5p mediates a positive feedback loop in EV71-induced apoptosis and suppresses virus replication.
414   *Sci. Rep.*, 7(1).

415 Zhou, F., Yu, T., Du, R., Fan, G., Liu, Y., Liu, Z., Xiang, J., Wang, Y., Song, B., Gu, X., et al. (2020a).
416   Clinical course and risk factors for mortality of adult inpatients with COVID-19 in Wuhan, China: a
417   retrospective cohort study. *Lancet*, 395(10229):1054–1062.

418 Zhou, P., Yang, X. L., Wang, X. G., Hu, B., Zhang, L., Zhang, W., Si, H. R., Zhu, Y., Li, B., Huang, C. L.,
419   et al. (2020b). A pneumonia outbreak associated with a new coronavirus of probable bat origin. *Nature*,
420   579(7798):270–273.

421 Zhuang, R. J., Bai, X. X., and Liu, W. (2019). MicroRNA-23a depletion promotes apoptosis of ovarian
422   cancer stem cell and inhibits cell migration by targeting DLG2. *Cancer Biol. Ther.*, 20(6):897–911.